

AFFACT - Alignment Free Facial Attribute Classification Technique

Manuel Günther,* Andras Rozsa,* and Terrance E. Boulton

Vision and Security Technology (VAST) Lab,
University of Colorado Colorado Springs
{mgunther, arozza, tboult}@vast.uccs.edu
* authors with equal contribution

Abstract— In this paper, we investigate how the latest versions of deep convolutional neural networks perform on the facial attribute classification task. We test two loss functions to train the neural networks: the sigmoid cross-entropy loss usually used in multi-objective classification tasks, and the Euclidean loss normally applied to regression problems, and find that there is little difference between these two loss functions. Rather, more attention should be paid on pre-training the network with external data, the learning rate policy and the evaluation technique. Using an ensemble of three ResNets, we obtain the new state-of-the-art facial attribute classification error of 8.00 % on the aligned images of the CelebA dataset. More significantly, we introduce a novel data augmentation technique allowing to train the AFFACT network that classifies facial attributes without requiring alignment, but works solely on detected face bounding boxes. We show that this approach outperforms the CelebA baseline, which did not use any face alignment either, with a relative improvement of 34 %.

I. INTRODUCTION

Unlike most other facial features used in recognition tasks, facial attributes have the unique property that they have a *semantic meaning* that can be interpreted by humans. This allows for applications using descriptive searches (e.g., “Caucasian female with blond hair”) [9], [11], [21] and might be interesting for forensic use, i.e., when eye witnesses describe suspects with such attributes. After Kumar *et al.* [10] showed that facial attributes are an interesting approach for face recognition, researchers have shifted their attention towards the task of automatic facial attribute prediction.

Deep convolutional neural networks (DCNNs) have become the *quasi standard* for handling almost *any kind of* image recognition or classification task. This includes generic image classification [13], [8], face recognition [24], [16] and facial landmark detection [27], [17]. Also, facial attribute classifiers have been advanced using DCNNs [14], [18], [20], [25], mostly leveraging the fact that Liu *et al.* [14] have provided a large-scale facial attribute dataset. While their algorithm still relies on external training data and additional SVM classifiers [14], it was shown that end-to-end facial attribute prediction systems [20], [25] can outperform their baseline without requiring additional training data [18], [20]. However, approaches in [18], [20], [25] used (hand-annotated) landmark locations, while [14] did not make use of facial landmarks. Given that attributes generally cover much larger regions of the image, it is reasonable to ask whether using aligned images is presuming a solution to a harder problem, i.e., facial landmark localization, in order to solve easier ones, i.e., facial attribute classification.



Fig. 1: ALIGNMENT FREE FACE IMAGE PROCESSING. *Imagine a deep convolutional neural network that can handle facial images without alignment. Only a dream? Using our new data augmentation technique we obtain the AFFACT network. For the displayed images, AFFACT classifies 35 to 40 out of 40 facial attributes correctly!*

Data augmentation has been shown to be a valid and useful way to increase the size of the training set without collecting additional training data [6], [2]. Traditionally, data augmentation is performed using simple techniques such as using several crops from an image and their horizontally mirrored versions [6]. Other approaches include adding random or non-random noise [19], and contrast or color modifications [2]. Including such transformations during training, the resulting DCNNs become more stable against those transformations. However, little research has been done on using different kinds of data augmentation such as rotation or scaling [15].

As shown [4], [16], face recognition works better when faces are aligned. Therefore, for most face processing tasks, the first step is to align the face based on facial landmarks in order to extract features from it [24], [25]. However, if no hand-labeled facial landmarks are provided or the automatic landmark detection fails – even for only a few relevant landmarks – faces cannot be aligned correctly and the recognition will fail, even though the face has been

detected. In this paper, we show that there is no need to align faces because we can use our alignment free facial attribute classification technique (AFFACT) to reliably predict facial attributes based on faces cropped using only detected bounding boxes.

Lately, new network topologies were developed [5] that are faster to train and more accurate. Also, the application of different training regimes [8] and loss functions, as well as ensembles of networks can lead to further advancements. Which of these advances are important for facial attribute prediction? In this paper, we:

- show that the state of the art in attribute classification can be improved by using the latest trends in DCNNs;
- provide an in-depth evaluation of different loss functions;
- introduce a new training regime that improves the robustness of facial attribute extraction;
- demonstrate that AFFACT can reliably predict facial attributes from images without alignment; and
- propose to use several crops of the image to make facial attribute extraction more reliable.

II. RELATED WORK

The application of perturbations or distortions to inputs to improve learning models has a long history in machine learning. Perturbations were applied to the MNIST dataset [12] and this technique has become a general training methodology [22]. Loosly *et al.* [15] developed an open source tool called InfMNIST that produces a perturbation-enhanced training set by applying small affine transformations and noise to original MNIST samples. Krizhevsky *et al.* [8] introduced three types of data augmentation techniques to improve the performance of their network on image classification. First, randomly located crops are taken from down-sampled original inputs, which makes the network more translation invariant. Second, to capture reflection invariance, training images are horizontally flipped. Finally, intensities of the RGB channels are randomly altered, in order to be more invariant to changes in lighting and color of the illumination. Chatfield *et al.* [2] demonstrated that data augmentation methods, commonly applied in deep learning, can significantly improve the performance of shallow representations as well. Howard [6] presented that additional data transformations used during testing can further improve deep neural network based image classification.

Recent approaches to classify facial attributes leverage deep convolutional neural networks (DCNNs). Liu *et al.* [14] combined three networks to first localize faces with two LNetS and then extract features using ANet on proposed face-locations that are finally fed into independent linear SVMs to obtain the final attribute classifications. Their attribute network (ANet) was first trained with external data for identification and then fine-tuned using facial attributes. Rozsa *et al.* [18] trained forty DCNNs, one for every single facial attribute, on the CelebA dataset and directly used the outputs of the trained networks for facial attribute classification. This

approach does not require secondary classifiers, still, outperforms LNetS+ANet by a large margin. Wang *et al.* [25] used an external dataset without manual identity labels to pre-train a network, that is later fine-tuned to perform attribute classification. Finally, Rudd *et al.* [20] introduced the mixed objective optimization network (MOON) that is able to both classify all facial attributes with a single learning model and supports domain adaptation, i.e., when distribution of training and operational test data differs. This approach is the current state of the art on the CelebA dataset.

III. APPROACH

In this paper, we focus on the multi-task problem of facial attribute classification via a single convolutional neural network. This section contains various approaches and techniques to further advance state-of-the-art attribute recognition on the CelebA benchmark, and to obtain learning models that better suit real-world applications.

A. Learning Models

Since the current state-of-the-art facial attribute classification accuracy on the CelebA dataset was achieved by the MOON architecture [20] built upon the 16-layer VGG model [23], we ask whether applying the latest, more advanced network topologies can lead to further improvements.

In general, deeper convolutional neural networks become more difficult to train, which limits the depth of our learning models and, implicitly, their performance as well. The introduction of the residual learning framework by He *et al.* [5] allows for training substantially deeper networks than previously used. The resultant deep residual networks (ResNets) are “easy” to be optimized – especially considering their increased depth – and have achieved excellent performances on various tasks. With respect to practical considerations, it is also important to notice that residual networks (with either 50, 101, or 152 layers) are faster than VGG models, both during training and testing. This is simply due to fact that residual networks have fewer filters and lower complexities.

Overall, residual networks have the potential to both achieve better performances and obtain learning models that are more practical for real-world applications. Here, we use two different network topologies, both based on the ResNet-50 model [5]. In the first case, we train a new ResNet-50 model using only the CelebA training images and reducing the last fully connected layer to 40 output units – the number of attributes in CelebA. In a second set of experiments, we investigate whether additional generic training data helps in learning attribute classification. We obtained a ResNet-50 model that was pre-trained on ImageNet for generic image classification. After adding an additional randomly initialized fully-connected layer with 40 output neurons, we fine-tuned that network using training images from CelebA. We refer to this network topology as ResNet-51.

B. Objective Functions for Multi-Label Training

To obtain the current state-of-the-art facial attribute recognition results on the CelebA dataset with their mixed objective optimization network (MOON), Rudd *et al.* [20] used

an Euclidean loss function, which mixes errors of all facial attributes. Rozsa *et al.* [18] also chose Euclidean loss to train DCNNs – one for every single facial attribute – following their intuition that facial “attributes lie along a continuous range, while sigmoids tend to enforce saturation and hinge-loss enforces a large margin”.

However, Euclidean loss is generally used for regression problems in machine learning, but facial attributes recognition is rather a classification task. Hence, we also apply a more traditional choice for classification tasks, i.e., sigmoid cross-entropy loss. To determine, which of the loss functions provide networks with better classification capabilities, we evaluate both Euclidean and sigmoid cross-entropy loss on the same dataset using the same network topologies.

For either of the two loss functions, networks are trained with a final fully-connected layer with 40 outputs – the number of attributes in CelebA. Like in [20], the final classification of the attribute is obtained by thresholding the corresponding network output at 0, i.e., positive or negative values correspond to the presence or absence of that attribute, respectively. We report classification errors per attribute on the CelebA test set. For easier comparison, we also average classification errors over all 40 attributes.

C. Training with Manually Adjusted Learning Rate

Similarly to [8], we adjust the learning rate manually throughout training by following a slightly modified heuristic. Starting with a relatively high learning rate of $\lambda = 10^{-3}$, the network is trained until the validation error stopped improving. Using the model with the lowest validation set error, we reduce the learning rate by a factor of 10 and continue training. We iterate these steps until we cannot observe further improvement on the validation set, usually the best model is obtained with a learning rate of $\lambda = 10^{-5}$.

This training approach – manually adjusted learning rates and hand-picked models for fine-tuning – can allow us to apply higher learning rates in the initial phase than would be possible otherwise. The intuition behind this “aggressive” training is simple. While starting the training with a relatively high learning rate might lead to fluctuating validation errors, the optimization algorithm has also a better chance to escape from local minima and reach a better minimum.

D. Data Augmentation for Training

For face image processing, usually the first step of the processing chain is to detect the face and facial landmarks in order to align the face. However, in difficult imaging conditions, any of these two steps can fail. In this paper, we focus on the question, what happens when the face is detected correctly – at least in a given range – but the facial landmark detection fails? Can we use the detected bounding boxes to extract the face and still get a decent facial attribute classification accuracy, even if the scale of the bounding box is incorrect, or the face is rotated in and out of plane?

To answer these questions, we introduce our new alignment free facial attribute classification technique (AFACT). We extend the traditional data augmentation technique to also

incorporate scaling and rotation of the image during training. Given a set of training images, which has annotated labels for both the attributes and for some facial landmarks [14], we align the face after applying some random modifications to the scale, the angle, and the location of the bounding box. Specifically, given the labels of the two eyes $\vec{t}_{e_r}, \vec{t}_{e_l}$ and the mouth corners $\vec{t}_{m_r}, \vec{t}_{m_l}$ with $\vec{t} = (x, y)^T$, we first compute the center of both and their respective distance d :

$$\vec{t}_e = \frac{\vec{t}_{e_r} + \vec{t}_{e_l}}{2} \quad \vec{t}_m = \frac{\vec{t}_{m_r} + \vec{t}_{m_l}}{2} \quad d = \|\vec{t}_e - \vec{t}_m\|, \quad (1)$$

before estimating the bounding box coordinates (specifying left, top, right and bottom coordinates x_l, y_t, x_r, y_b):

$$\begin{aligned} x_l &= x_e - 0.5 \cdot w & x_r &= x_e + 0.5 \cdot w \\ y_t &= y_e - 0.45 \cdot h & y_b &= y_e + 0.55 \cdot h \end{aligned} \quad (2)$$

as well as the original rotation angle obtained from the eye locations:

$$\alpha = \arctan \frac{y_{e_r} - y_{e_l}}{x_{e_r} - x_{e_l}}. \quad (3)$$

The height h and width w of the bounding box are estimated based on the mouth-eye-distance: $h = w = 5.5 \cdot d$.

We have implemented a new data layer in the Caffe framework [7] that computes different random perturbations of bounding boxes for each training image in each training epoch, using Bob [1] to handle the image transformations and OpenMP [3] for parallelization on the CPU. This layer has the advantage that it can create training samples on the fly, without requiring to store them on hard disk. In this layer, original images and computed bounding boxes including angle α are loaded, the scale $s = \min W/w, H/h$ is estimated, offsets for angle $r_\alpha \sim \mathcal{N}_{0,20}$, shift $r_y, r_x \sim \mathcal{N}_{0,0.05}$ and scale $r_s \sim \mathcal{N}_{1,0.1}$ are randomly drawn and added to the coordinates:

$$\begin{aligned} \tilde{x}_l &= x_l + \tilde{r}_x \cdot w, & \tilde{x}_r &= x_r + \tilde{r}_x \cdot w, & \tilde{\alpha} &= \alpha + r_\alpha, \\ \tilde{y}_t &= y_t + \tilde{r}_y \cdot w, & \tilde{y}_b &= y_b + \tilde{r}_y \cdot w, & \tilde{s} &= s \cdot \tilde{r}_s. \end{aligned} \quad (4)$$

Using these coordinates, the image is rotated, scaled and cropped into an RGB image of resolution $W = H = 224$, and horizontally flipped with a chance of 50%. To emulate smaller image resolutions, which would result in a blurred upscaled image, a Gaussian filter with a random standard deviation of $\sigma \sim \mathcal{N}_{0,3}$ is used to smooth the image, which is finally fed as input to the network training. Fig. 2 shows some examples of the training images cropped without and with random perturbations.

Note that all the parameters used above have been selected to suite the characteristics of the CelebA dataset and the facial attribute classification task. Particularly, the amount of scale, angle, shift and blur were adapted to work with the rotations of the faces in the CelebA dataset, as well as the quality of the face detector [17]. However, they might easily be adapted to work with other image resolutions, image content, and face detectors.

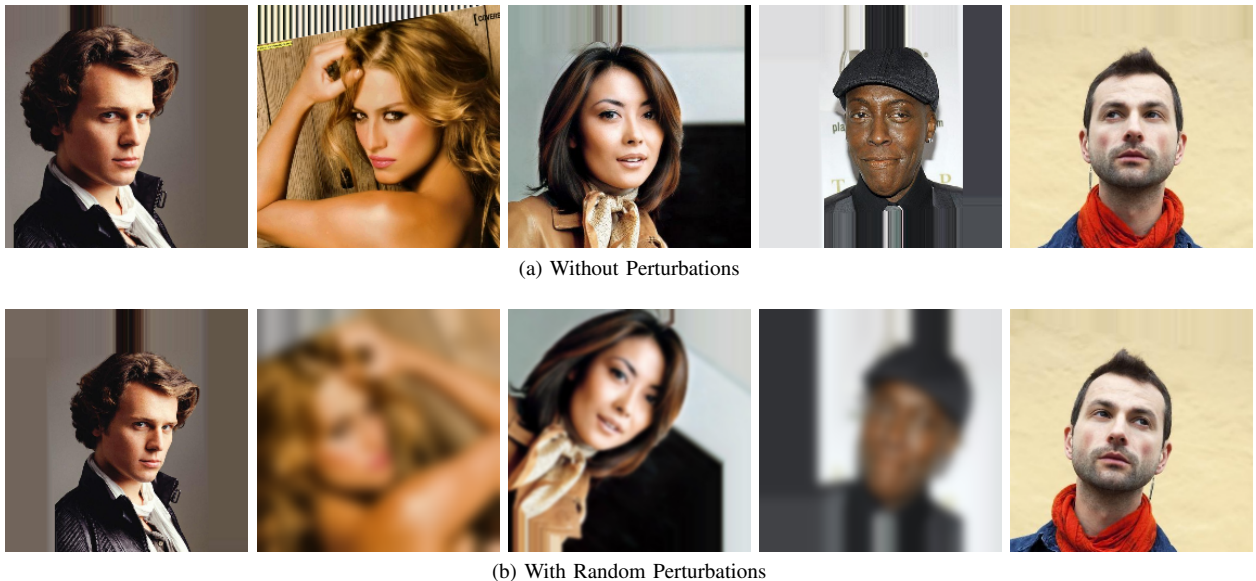


Fig. 2: RANDOMLY PERTURBED TRAINING IMAGES. This figure shows the impact of our random perturbations to image alignment. In (a), images are aligned using only the bounding box and angle, while (b) shows the same images with random scale, angle, shift, blur and horizontal flip.

E. Data Augmentation for Testing

Data augmentation can also be effectively used for testing in order to further enhance performances of DCNNs [6]. For instance, participants of the ImageNet challenge report error rates on the extracted center crops of original images – regardless of whether the actual object is partially present or not at all – and also apply various data augmentations to achieve better results. A common practice is to combine predictions of 10 transformations into a final prediction, i.e., using their average, by enlarging the image and taking the center crop together with crops of the four corners of the original and the horizontally flipped images. In our experiments, we adopt this strategy and rescale the test images to a resolution of 256×256 pixels before taking those 10 crops. We average the resulting DCNN output scores per attribute, and threshold the results at 0 to obtain the final attribute classification.

While this simple cropping technique proved to be beneficial in testing, it was demonstrated that additional transformations can lead to further advancements, such as applying cropping and predictions at multiple scales and/or with multiple views [6].

IV. EXPERIMENTS

A. Dataset

We conducted our experiments on the CelebA dataset [14], which consists of more than 200K images, with an average of 20 images of approximately 10K celebrities. Most of the images show a single face with a close-to-frontal pose, but some half-profile and few profile faces are included as well. The training set is formed by images of the first 8K identities and, therefore, contains 160K images. The remaining 2K identities are equally split into the validation and test set,

each having approximately 20K images. The dataset provides five key-points – both eyes, the mouth corners, and the nose tip – and binary labels of 40 facial attributes for each image. As ResNets were designed to work with 224×224 pixel images, we aligned images with that resolution by using the provided key-points.

In order to test how well networks perform on automatically detected facial images, we applied two different face detectors. First, the built-in face detector of Bob [1] was used to extract faces. As the face detector was trained on frontal images only and might not detect all faces reliably, we obtained several possible face locations and took the bounding box that overlapped the most with the hand-labeled locations. In this way, we do not miss many faces, still, we can test our networks on automatically detected faces.

To perform a fair comparison with the original LNet+ANet [14] approach that did not use hand-labeled annotations, we used the state-of-the-art face detector [17] on the full size images of the CelebA test set. We used only the detected bounding boxes, which we enlarged to approximately fit to the content used for training, see Fig. 2(a), and cropped the image to resolution 224×224 pixels. For the few images with multiple detections, we used the bounding box that had the largest overlap with the box derived from the ground-truth key-points. When the face detector had no detection – which happened in 40 of the 19962 CelebA test images – we scaled the smaller side of the image to 224 pixels and took the center crop.

B. Facial Attribute Classification on Aligned Images

We commenced our experiments with training and comparing residual networks on the aligned 224×224 images to find the most applicable network size with respect to the number of layers. We did not incorporate any form of

TABLE I: ATTRIBUTE CLASSIFICATION ERROR RATES. This table shows the achieved error rates for each attribute, separately. Networks are either tested on aligned images (A), 10 crops of aligned images (C) or automatically detected faces (D). For comparison, results of MOON [20] and LNet+ANet [14] are given on both sides of the table.

Tested on	MOON	ResNet-50-E	ResNet-50-S	ResNet-51-E	ResNet-51-S	ResNet-51-E Ensemble	AFFACT	ResNet-51-S	AFFACT	ResNet-51-S	AFFACT	AFFACT Ensemble	LNet+ANet
	A	A	A	A	A	A	A	C	C	D	D	CD	D*
5 o Clock Shadow	5.97	5.64	5.17	5.20	4.94	5.07	5.13	7.88	4.94	5.72	5.19	5.02	9
Arched Eyebrows	17.74	16.16	15.58	14.83	14.65	14.54	15.79	21.98	15.65	20.19	16.70	15.85	21
Attractive	18.33	17.26	16.97	16.75	16.63	16.39	17.14	19.54	16.95	20.25	17.20	17.01	19
Bags Under Eyes	15.08	14.72	14.39	14.25	14.08	13.95	14.69	19.09	14.27	17.30	15.09	14.83	21
Bald	1.23	1.16	1.03	0.88	0.94	0.89	0.91	1.06	0.97	1.04	0.96	0.96	2
Bangs	4.20	4.14	4.08	3.85	3.77	3.74	3.90	4.42	3.87	4.47	3.99	3.77	5
Big Lips	28.52	27.99	27.80	27.68	27.53	27.27	27.30	30.01	27.51	28.81	28.32	28.46	32
Big Nose	16.00	15.65	15.72	14.77	14.82	14.51	15.62	16.40	15.26	16.27	15.43	15.23	22
Black Hair	10.60	10.33	10.05	9.88	9.59	9.71	9.64	10.27	9.44	10.49	9.73	9.44	12
Blond Hair	4.14	4.02	4.09	4.07	4.09	4.00	3.80	3.90	3.82	4.15	3.96	3.77	5
Blurry	4.33	3.88	3.94	3.59	3.64	3.49	3.63	6.92	3.62	4.81	3.90	3.91	16
Brown Hair	10.62	10.29	10.83	10.28	10.61	10.23	11.60	10.63	10.89	11.24	11.92	10.81	20
Bushy Eyebrows	7.38	7.06	7.06	7.21	7.27	7.02	7.54	11.34	7.60	10.57	7.52	7.16	10
Chubby	4.56	4.47	4.44	4.15	4.37	4.09	4.26	4.46	4.20	4.73	4.30	4.25	9
Double Chin	3.68	3.65	3.65	3.45	3.58	3.37	3.48	3.65	3.60	3.94	3.57	3.54	8
Eyeglasses	0.53	0.34	0.31	0.27	0.32	0.29	0.39	0.66	0.32	0.55	0.41	0.36	1
Goatee	2.96	2.57	2.69	2.37	2.29	2.24	2.50	2.89	2.45	2.66	2.44	2.35	5
Gray Hair	1.90	1.71	1.88	1.66	1.58	1.62	1.69	1.58	1.61	1.73	1.70	1.62	3
Heavy Makeup	9.01	8.45	8.17	7.94	7.83	7.77	7.90	9.56	7.74	11.06	8.17	7.94	10
High Cheekbones	12.99	12.37	12.34	11.97	11.90	11.73	12.23	21.58	12.20	15.32	12.77	12.20	13
Male	1.90	1.93	1.88	1.67	1.66	1.50	1.50	2.58	1.49	2.66	1.77	1.65	2
Mouth Slightly Open	6.46	6.21	6.05	5.98	5.76	5.93	5.94	12.29	5.79	9.09	6.22	6.02	8
Mustache	3.18	2.95	2.87	2.78	2.73	2.79	2.89	3.62	2.88	3.22	2.86	2.92	5
Narrow Eyes	13.48	12.42	12.12	12.36	12.12	12.22	12.31	12.84	12.28	13.47	12.60	12.33	19
No Beard	4.42	3.93	3.73	3.51	3.53	3.36	3.55	5.46	3.47	4.31	3.60	3.66	5
Oval Face	24.27	23.19	23.31	22.15	22.12	21.66	22.59	26.11	22.67	25.92	25.22	23.89	34
Pale Skin	3.00	2.91	2.90	2.95	2.75	2.85	2.95	2.99	2.78	2.93	2.82	2.68	9
Pointy Nose	23.54	22.69	22.96	22.01	22.43	21.96	23.10	24.82	22.65	24.18	22.88	22.06	28
Receding Hairline	6.44	6.29	6.18	6.16	5.92	5.95	6.33	6.36	6.15	7.07	6.32	6.00	11
Rosy Cheeks	5.18	4.83	4.76	4.70	4.60	4.46	4.84	6.95	4.77	6.03	5.04	4.76	10
Sideburns	2.41	2.26	2.12	1.96	1.93	1.91	2.16	2.20	2.08	2.10	2.14	2.02	4
Smiling	7.40	7.12	7.01	6.64	6.83	6.51	7.04	13.68	6.65	11.79	7.22	6.96	8
Straight Hair	17.74	16.32	15.97	14.56	14.80	14.19	14.74	15.76	14.67	15.03	14.77	14.43	27
Wavy Hair	17.53	17.05	15.30	14.38	14.70	13.69	13.75	15.80	14.03	15.07	13.93	14.10	20
Wearing Earrings	10.40	9.74	9.36	8.87	9.02	8.84	9.02	10.55	8.96	9.55	9.08	8.96	18
Wearing Hat	1.05	0.98	0.86	0.87	0.82	0.84	0.90	0.86	0.83	1.02	0.86	0.91	1
Wearing Lipstick	6.07	6.03	6.21	5.77	5.93	5.62	6.04	8.40	6.07	8.16	5.95	5.91	7
Wearing Necklace	12.96	11.85	11.50	10.61	10.59	10.40	10.73	12.08	11.38	10.86	11.16	11.69	29
Wearing Necktie	3.37	3.04	2.82	2.74	2.71	2.72	2.71	3.88	2.77	2.85	2.84	2.74	7
Young	11.92	11.89	11.68	11.18	11.17	10.83	11.02	11.91	11.03	12.12	11.35	11.27	13
OVERALL	9.06	8.64	8.49	8.17	8.16	8.00	8.33	10.17	8.26	9.57	8.55	8.34	12.7

data augmentation during training. After experimenting with residual networks having either 18, 32, 50, or 101 layers, we found that 50-layer network provides the best results. The employed ResNet-50 network architecture is fully based upon the model of [5], we only modified the outputs of the last fully connected layer to match the 40 facial attributes.

We trained ResNet-50 models using Euclidean or sigmoid cross-entropy loss functions, using the same hyperparameters. The effective batch-size was set to 64 images, therefore, one epoch requires approximately 2.5K iterations. We chose an RMSProp update rule with inverse learning rate decay policy and applied manually adjusted learning rates as described in Sec. III-C, with an initial value of $\lambda = 10^{-3}$.

After training 3 networks for each objective function, we selected the network with the lowest loss on the validation set. As shown in Tab. I, ResNet-50 models trained with either Euclidean (ResNet-50-E) or sigmoid cross-entropy (ResNet-50-S) loss lead to better performing networks than the cur-

rent state-of-the-art architecture (MOON). We can observe that ResNet-50-S (8.49 %) slightly outperforms ResNet-50-E (8.64 %), and for both, the classification error is significantly better than MOON (9.06 %) [20]. The obtained relative improvement of ResNet-50-S over MOON is presented in Fig. 3 for all facial attributes separately.

Although we already achieved excellent results by training networks only on the CelebA training set, we ran further experiments. It is well known that initializing a network with transferred features – even from very dissimilar tasks – can result in better generalization than starting from random features [26]. Therefore, we also adjusted residual networks initialized with features of the ResNet-50 model optimized on the ImageNet dataset.¹ In order to utilize all learnt features, we modified the original 50-layer architecture by adding an extra fully connected layer with 40 outputs. We

¹We obtained the pre-trained 50-layer residual network from <http://github.com/KaimingHe/deep-residual-networks>

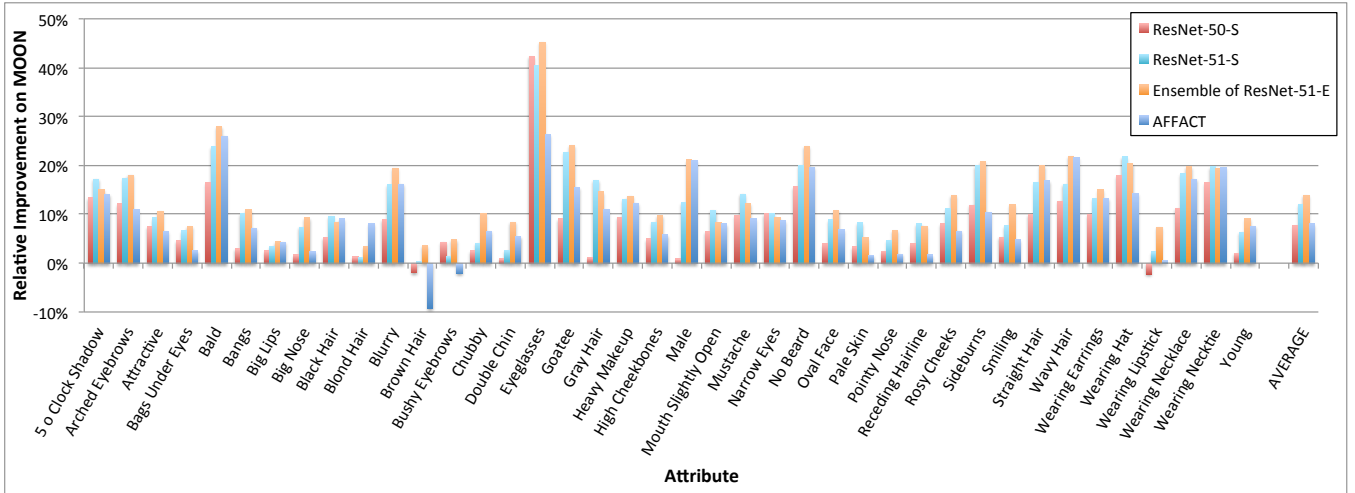


Fig. 3: RELATIVE IMPROVEMENT ON MOON. This figure shows the achieved relative improvements of several of our tested networks over MOON [20], for each attribute separately. All networks are evaluated on aligned images.

refer to this model as ResNet-51. For comparison, we fine-tuned ResNet-51 networks – pre-trained on ImageNet – with Euclidean loss and sigmoid cross-entropy loss as well. We used an initial learning rate of 10^{-4} , otherwise we applied the same hyper-parameters as before. Similarly to previous experiments, we trained 3 networks with each objective function and selected the one with the lowest loss on the validation set. We can see in Tab. I that this approach yields better results. While optimizing with Euclidean loss (ResNet-51-E) leads to 8.17% overall error rate, applying sigmoid loss results in our best performing network (ResNet-51-S) with 8.16% classification error rate on the CelebA dataset – a 9.9% relative improvement over the current state of the art. The per-attribute relative improvement achieved by ResNet-51-S over MOON is shown in Fig. 3.

As an attempt to further advance the overall performance, we also conducted experiments using ensembles of networks, and applying test data augmentation. An ensemble is the application of multiple learning models to obtain better performance by combining their predictions. We observed that by forming ensembles of our 3 fine-tuned residual networks – optimized either with Euclidean or sigmoid cross-entropy loss – we can improve over the best classification error rate that we achieved with a single DCNN. The results that we obtained are very similar for both loss functions: 8.00% with Euclidean (cf. Tab I), and 8.01% overall error rate using sigmoid cross-entropy loss, both yielding 11.7% relative improvement over MOON. Considering the gain over single networks, the application of ensembles has a good potential to boost the overall performance.

Since data transformations applied during testing can improve the overall performance of DCNNs, we also tested our trained models on 10 crops of test images as described in Sec. III-E. After re-scaling the test images to 256×256 pixels, we extracted five crops, horizontally flipped them, and used the average network output as the final prediction. Surprisingly, we experienced a significant degradation

in classification error rates as they increased to $>10\%$. For example, ResNet-51-S suffered an approximately 2% degradation in overall error rate when we tested on 10 crops, as shown in Tab. I, and ResNet-50-E increased to over 14% error. Even the smallest data transformations – using 225×225 pixel images for initial re-scaling – lead to increased error rates. While this phenomenon can be explained as the result of training with aligned images, it also highlights that these DCNNs are sensitive to even the smallest misalignment and, therefore, their performances highly depend on facial landmark detection.

C. Face Alignment? Who Cares!

What we need is a network that is more stable against reasonable variations in scale, angle, and location of the face in the extracted image, and also capable of extracting attributes from a range of image resolutions. We took the best performing network from above, i.e., ResNet-51-S, but this time we trained the DCNN using the data augmentation technique as described in Sec. III-D. We call this approach the Alignment Free Facial Attribute Classification Technique (AFFACT). Despite the training set augmentation, we used the exact same training technique as before. For the validation set, instead of using aligned faces, we employed images based on the cropped bounding box, which is computed with Eq. (2) without random perturbations and with $\alpha = 0$.

In order to verify that we did not give up on accuracy on the aligned faces, we tested our AFFACT network on the aligned test images as used before. The results are listed in Tab. I. As we can see, compared to the base ResNet-51-S the overall error rate slightly increased from 8.16% to 8.33%. For most attributes the error increased with the same amount, but, interestingly, for some attributes that are affected by larger parts of the face such as Blond Hair, Male, or Young, AFFACT can even achieve better results than ResNet-51-S.

The goal of training with our data augmentation technique is to make the AFFACT network less dependent on face

alignment. Ideally, this would help attribute classification in two different ways. First, we would be able to use image crops that failed miserably on the aligned images in the last section. Second, we could use faces detected by a face detector, where fiducial detection fails or is imprecise.

Indeed, when applying the same 10 crops as in the previous section, the AFFACT network improves accuracy – the error rates given in Tab. I are comparable to the ones of ResNet-51-S on aligned images without crops. Theoretically, there is a chance to further improve the results by not only cropping different regions of the face image, but using different scales and rotation angles. We leave to test these assumptions to future work.

The most impressive characteristic of the AFFACT network is its robustness to facial misalignment. As a first test, we evaluated both the AFFACT and the ResNet-51-S network on images that were cropped based on Bob’s face detector, where we made sure that all faces were detected. Compared to the aligned images, the main difference is that some faces are not upright or not fully centered in the images, which occurs only a few times in the CelebA test set. While the overall error of the ResNet-51-S network increased from 8.16 % to 8.82 %, the AFFACT result of 8.48 % is approximately stable compared to the 8.33 % on the aligned faces. In Fig. 1, we show some examples where the total number of correct attribute classifications between ResNet-51-S and AFFACT differs. Specifically, we can see images where AFFACT was able to classify seven to nine more attributes correctly than ResNet-51-S – between 35 and 40 of the attributes are classified correctly by AFFACT for those images. Interestingly, all of these images show medium to large in-plane rotations of the face, and two faces are not in the center of the image, showing that AFFACT is stable against rotations and translations. On the other hand, when the total number of more correctly classified attributes is in the advantage of ResNet-51-S, all of those images are very upright and well centered in the image (not shown here).

Finally, we compared the results of the two networks on actual face detections obtained with the state-of-the-art face detector from Ranjan *et al.* [17]. These results are now directly comparable with the LNet+ANet approach [14], which also did not use facial landmarks in their experiments and reached an average classification error of 12.70 % [20]. As seen in Tab. I, the results of both networks deteriorated, which is mainly due to the fact that some of the faces were not detected correctly, i.e., parts of the faces were not inside the image. Although the 9.57 % error rate of ResNet-51-S is already better than the 12.70 % of LNet+ANet, this is radically outperformed by 8.55 % of AFFACT. Looking at the values for single attributes, we can observe that the main advantage of AFFACT over ResNet-51-S on detected faces is in highly localized attributes, such as Arched Eyebrows, Bushy Eyebrows, Heavy Makeup, Mouth Slightly Open, or Smiling.

Finally, when combining all methods investigated in this paper, i.e., using an ensemble of three AFFACT networks and averaging over 10 crops of the detected bounding boxes,

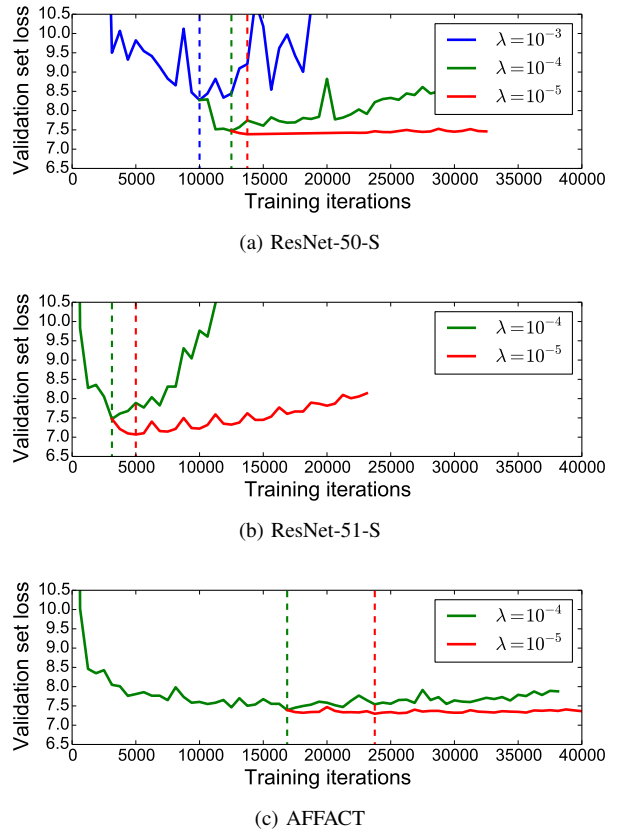


Fig. 4: VALIDATION SET ERRORS. This figure shows the trends of the validation loss obtained during the multi-stage training of (a) ResNet-50-S, (b) ResNet-51-S, and (c) AFFACT. Dotted lines mark the lowest validation set loss for that learning rate.

we can lower the classification error to 8.34 % (see Tab. I), which represents the new state of the art on the CelebA benchmark using detected faces without alignment, with a relative improvement of 34.0 % over LNet+ANet [14].

V. CONCLUSIONS

In this paper, we obtained the new state of the art in facial attribute classification on the CelebA [14] benchmark, i.e., classification errors of 8.00 % on aligned images and 8.34 % on detected faces. The achieved relative improvements over the previous state of the art are 11.7 % over MOON [20] and 34.0 % over LNet+ANet [14], respectively.

The results on aligned faces were achieved by using an ensemble of three ResNet-51-S networks that were pre-trained on the ImageNet image classification task, and fine-tuned using the CelebA training images. We also tried to train those networks purely on the CelebA training set, but found that those networks result in slightly lower training speeds and accuracies. We obtained our results by applying a different learning rate strategy, i.e., by decreasing learning rates by a factor of 10, when the validation loss stops improving. To show the effectiveness of this approach, we show the validation set losses during training in Fig. 4, for the three stages of ResNet-50-S and the two stages of both ResNet-51-S and AFFACT. Using this strategy, we also re-trained the

MOON network and obtained 8.67 % average classification error. When starting the learning rate $\lambda = 10^{-5}$, we did not achieve such good results in any of our network trainings. We also tested two different loss functions – the sigmoid cross-entropy loss and the Euclidean loss – and found that there is little difference in terms of classification error.

To obtain the result on detected faces, we developed a new data augmentation technique: AFFACT. We showed that – on the cost of a moderately increased training time – the AFFACT network is able to use the detected bounding boxes provided by a face detector without further alignment to classify facial attributes. Nevertheless, our novel data augmentation technique is generic and can be easily adapted to other face processing tasks, e.g., face recognition. We will investigate on this in our future work.

We experimented with several crops of the images in order to improve attribute classification. However, for the ResNet-51-S network that was trained on aligned images, the classification error surprisingly increased. On the other hand, the AFFACT network was able to utilize several crops of the face to further improve attribute classification. To date, we only used several crops of the faces to improve accuracy. When the original face was misaligned, we might not have the best position, scale or angle to extract attribute information reliably. An interesting question is whether a different kind of cropping, i.e., incorporating rotation and scaling into the test image preparation would help to improve or stabilize attribute predictions.

As indicated by [20], training end-to-end systems using a biased dataset might influence the distributions of positive and negative classification errors. Further research would be required to test whether this bias is also present in the AFFACT network, and whether the same balancing technique would work to counter that. Another related question is how well these new attribute predictions work, e.g., in a face recognition task, and whether the proposed training and test augmentation techniques would be useful for that task. These questions will be addressed by future work.

Lately, we realized that a lot of images in the CelebA dataset have wrong attribute labels. We are currently in the process of relabeling those errors. We assume that the real classification errors are at least 25 % lower than reported in literature and this paper.

ACKNOWLEDGMENT

This research is based upon work supported in part by NSF IIS-1320956 and in part by the Office of the Director of National Intelligence (ODNI), Intelligence Advanced Research Projects Activity (IARPA), via IARPA R&D Contract No. 2014-14071600012. The views and conclusions contained herein are those of the authors and should not be interpreted as necessarily representing the official policies or endorsements, either expressed or implied, of the ODNI, IARPA, or the U.S. Government. The U.S. Government is authorized to reproduce and distribute reprints for Governmental purposes notwithstanding any copyright annotation thereon.

REFERENCES

- [1] A. Anjos, L. E. Shafey, R. Wallace, M. Günther, C. McCool, and S. Marcel. Bob: a free signal processing and machine learning toolbox for researchers. In *20th ACM Conference on Multimedia Systems (ACMMM)*, Nara, Japan. ACM Press, Oct. 2012.
- [2] K. Chatfield, K. Simonyan, A. Vedaldi, and A. Zisserman. Return of the devil in the details: Delving deep into convolutional nets. In *Proceedings of the British Machine Vision Conference (BMVC)*, 2014.
- [3] L. Dagum and R. Menon. Openmp: An industry-standard api for shared-memory programming. *IEEE Comput. Sci. Eng.*, 5(1):46–55, Jan. 1998.
- [4] A. Dutta, M. Günther, L. El Shafey, S. Marcel, R. Veldhuis, and L. Spreeuwers. Impact of eye detection error on face recognition performance. *IET Biometrics*, 4:137–150, 2015.
- [5] K. He, X. Zhang, S. Ren, and J. Sun. Deep residual learning for image recognition. In *Proceedings of the IEEE Conference on Computer Vision and Pattern Recognition (CVPR)*, 2016. arXiv preprint arXiv:1512.03385.
- [6] A. G. Howard. Some improvements on deep convolutional neural network based image classification. In *International Conference on Learning Representation (ICLR)*, 2014. arXiv preprint arXiv:1312.5402.
- [7] Y. Jia, E. Shelhamer, J. Donahue, S. Karayev, J. Long, R. Girshick, S. Guadarrama, and T. Darrell. Caffe: Convolutional architecture for fast feature embedding. *arXiv preprint arXiv:1408.5093*, 2014.
- [8] A. Krizhevsky, I. Sutskever, and G. E. Hinton. Imagenet classification with deep convolutional neural networks. In *Advances in Neural Information Processing Systems (NIPS)*, pages 1097–1105, 2012.
- [9] N. Kumar, P. Belhumeur, and S. Nayar. FaceTracer: A Search Engine for Large Collections of Images with Faces. In *European Conference on Computer Vision*, pages 340–353. Springer, 2008.
- [10] N. Kumar, A. C. Berg, P. N. Belhumeur, and S. K. Nayar. Attribute and Simile Classifiers for Face Verification. In *International Conference on Computer Vision*, pages 365–372. IEEE, 2009.
- [11] N. Kumar, A. C. Berg, P. N. Belhumeur, and S. K. Nayar. Describable Visual Attributes for Face Verification and Image Search. *IEEE Transactions on Pattern Analysis and Machine Intelligence*, 33(10):1962–1977, 2011.
- [12] Y. LeCun, C. Cortes, and C. J. Burges. The mnist database of handwritten digits, 1998.
- [13] Y. LeCun, L. Jackel, L. Bottou, C. Cortes, J. S. Denker, H. Drucker, I. Guyon, U. Muller, E. Sackinger, P. Simard, et al. Learning algorithms for classification: A comparison on handwritten digit recognition. *Neural networks: the statistical mechanics perspective*, 261:276, 1995.
- [14] Z. Liu, P. Luo, X. Wang, and X. Tang. Deep learning face attributes in the wild. In *Proceedings of the IEEE International Conference on Computer Vision*, pages 3730–3738, 2015.
- [15] G. Loosli, S. Canu, and L. Bottou. Training invariant support vector machines using selective sampling. *Large scale kernel machines*, pages 301–320, 2007. Project InfiMNIST available at <http://leon.bottou.org/projects/infimnist> Accessed on September 8, 2016.
- [16] O. M. Parkhi, A. Vedaldi, and A. Zisserman. Deep Face Recognition. *British Machine Vision Conference*, 1(3):6, 2015.
- [17] R. Ranjan, V. M. Patel, and R. Chellappa. Hyperface: A deep multi-task learning framework for face detection, landmark localization, pose estimation, and gender recognition, 2016. under review.
- [18] A. Rozsa, M. Günther, E. M. Rudd, and T. E. Boulton. Are facial attributes adversarially robust? In *International Conference on Pattern Recognition (ICPR)*, 2016.
- [19] A. Rozsa, E. M. Rudd, and T. E. Boulton. Adversarial diversity and hard positive generation. In *The IEEE Conference on Computer Vision and Pattern Recognition (CVPR) Workshops*, June 2016.
- [20] E. M. Rudd, M. Günther, and T. E. Boulton. MOON: A mixed objective optimization network for the recognition of facial attributes. In *European Conference on Computer Vision (ECCV)*, 2016.
- [21] W. J. Scheirer, N. Kumar, P. N. Belhumeur, and T. E. Boulton. Multi-Attribute Spaces: Calibration for Attribute Fusion and Similarity Search. In *Conference on Computer Vision and Pattern Recognition*, pages 2933–2940. IEEE, 2012.
- [22] P. Y. Simard, D. Steinkraus, and J. C. Platt. Best practices for convolutional neural networks applied to visual document analysis. In *Document Analysis and Recognition, 2003. Proceedings. Seventh International Conference on*, pages 958–963. IEEE, 2003.
- [23] K. Simonyan and A. Zisserman. Very deep convolutional networks

- for large-scale image recognition. In *Proceedings of the International Conference on Learning Representations (ICLR)*, 2015.
- [24] Y. Taigman, M. Yang, M. Ranzato, and L. Wolf. Deepface: Closing the gap to human-level performance in face verification. In *Proceedings of the 2014 IEEE Conference on Computer Vision and Pattern Recognition*, CVPR '14, pages 1701–1708, Washington, DC, USA, 2014. IEEE Computer Society.
- [25] J. Wang, Y. Cheng, and R. S. Feris. Walk and learn: Facial attribute representation learning from egocentric video and contextual data. In *Computer Vision and Pattern Recognition*. IEEE, 2016.
- [26] J. Yosinski, J. Clune, Y. Bengio, and H. Lipson. How transferable are features in deep neural networks? In *Advances in neural information processing systems*, pages 3320–3328, 2014.
- [27] Z. Zhang, P. Luo, C. C. Loy, and X. Tang. *Facial Landmark Detection by Deep Multi-task Learning*, pages 94–108. Springer International Publishing, 2014.